

# Supporting Information

## Magnetical hollow micro-sized nanoaggregates for synergistically accelerating PET glycolysis

Ling-Xia Yun<sup>a,b</sup>, Yan Wei<sup>a,b</sup>, Qian Sun<sup>c</sup>, Yu-Ting Li<sup>a,b</sup>, Bin Zhang<sup>a,b</sup>, Hang-Tian Zhang<sup>b,\*</sup>, Zhi-Gang Shen<sup>d</sup>, Jie-Xin Wang<sup>a,b,\*</sup>

<sup>a</sup>*State Key Laboratory of Organic-Inorganic Composites, Beijing University of Chemical Technology, Beijing 100029, PR China;*

<sup>b</sup>*Research Center of the Ministry of Education for High Gravity Engineering and Technology, Beijing University of Chemical Technology, Beijing, 100029, PR China;*

<sup>c</sup>*Guangxi Key Laboratory of Petrochemical Resource Processing and Process Intensification Technology and School of Chemistry and Chemical Engineering, Guangxi University, Nanning, 530004, PR China;*

<sup>d</sup>*School of Chemical Engineering, Xiangtan University, Xiangtan, Hunan, 411105*

Total number of pages: 10

Total number of Fig.s:13 (Fig.s S1-S13)

Total number of Tables:1 (Table S1)

---

\* Corresponding authors:

Hang-Tian Zhang, E-mail: [zhanghangtian\\_zemon@outlook.com](mailto:zhanghangtian_zemon@outlook.com) (H.T. Zhang)

Jie-Xin Wang, E-mail: [wangjx@mail.buct.edu.cn](mailto:wangjx@mail.buct.edu.cn) (J.X. Wang)

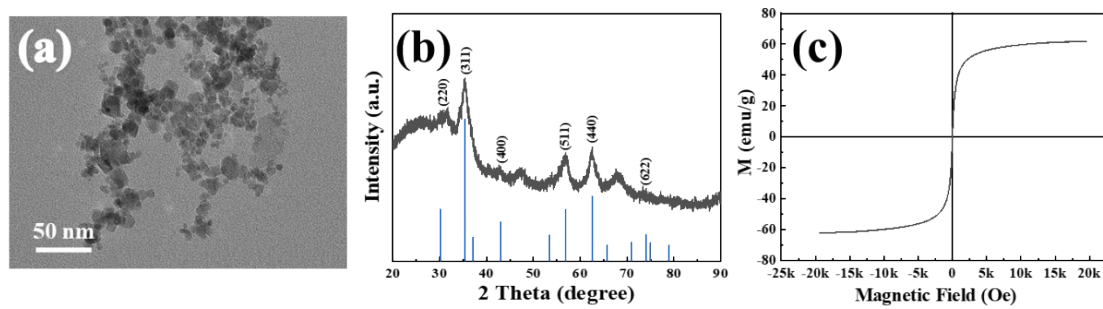


**Fig. S1.** (a) The TEM image, (b) XRD pattern and (c) hysteresis loop of Fe<sub>3</sub>O<sub>4</sub> NPs.

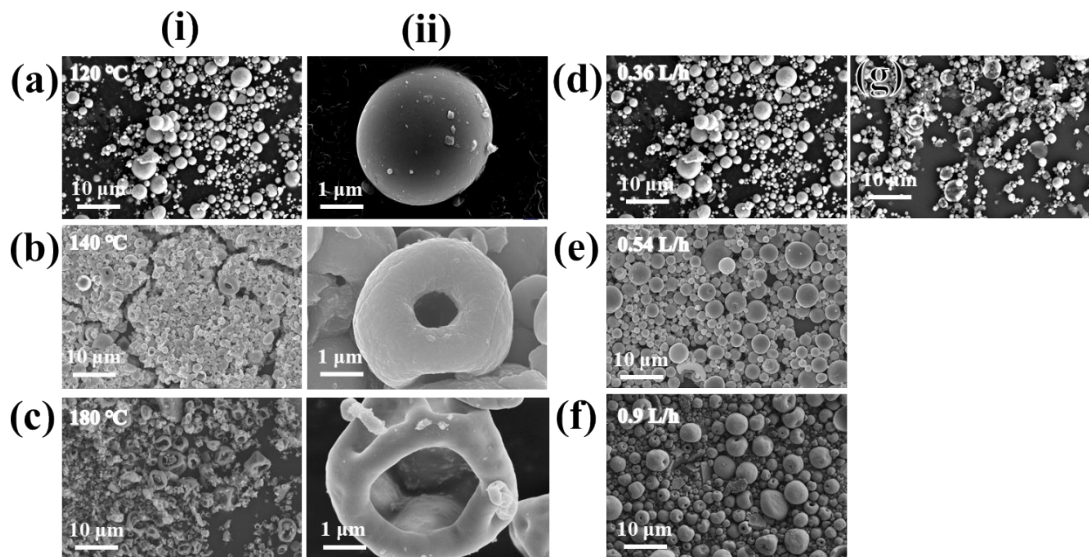


**Fig. S2.** SEM images of ZnO-3.5 nm-Fe<sub>3</sub>O<sub>4</sub> HMNAs obtained under different inlet temperatures: (a) 120 °C, (b) 140 °C, (c) 180 °C and different feed rates: (d) 0.36 L/h, (e) 0.54 L/h, (f) 0.9 L/h. (g) The SEM image of cracked hollow microspheres after the ultrasound treatment for a period of time.

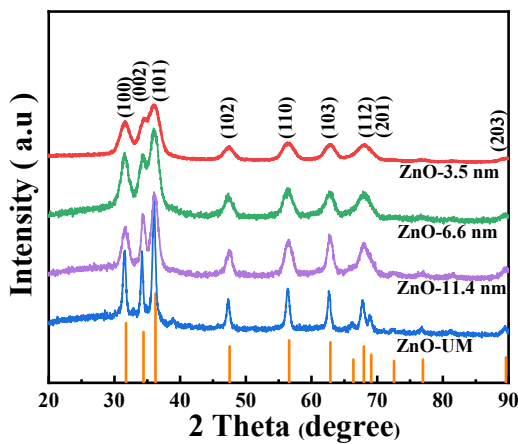


**Fig. S3.** XRD patterns of obtained ZnO NPs.

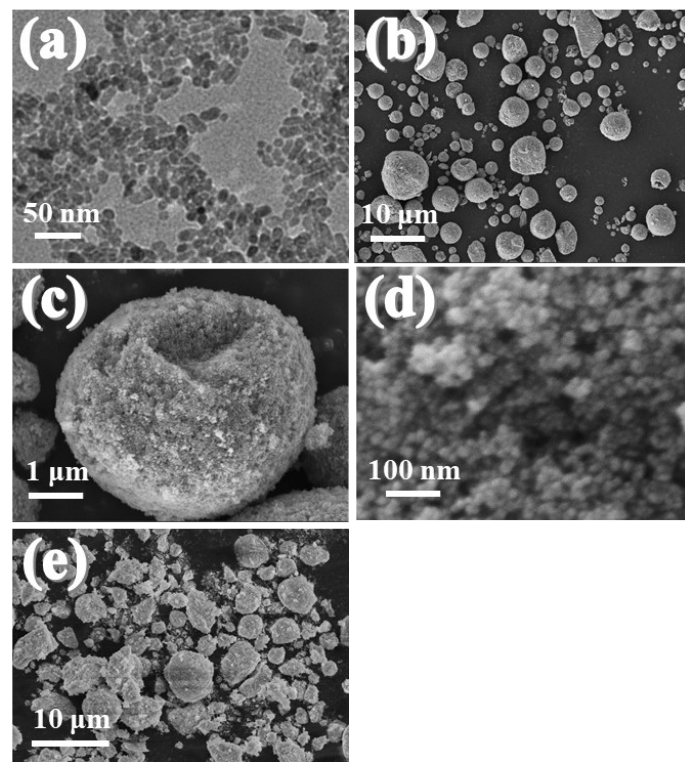


**Fig. S4.** (a) TEM images of the ZnO-UM suspension. (b-d) SEM images of the ZnO-UM-Fe<sub>3</sub>O<sub>4</sub>-2:1 HMNAs. (e) The SEM image of ZnO-Fe<sub>3</sub>O<sub>4</sub> particles obtained from poorly dispersed ZnO powder.

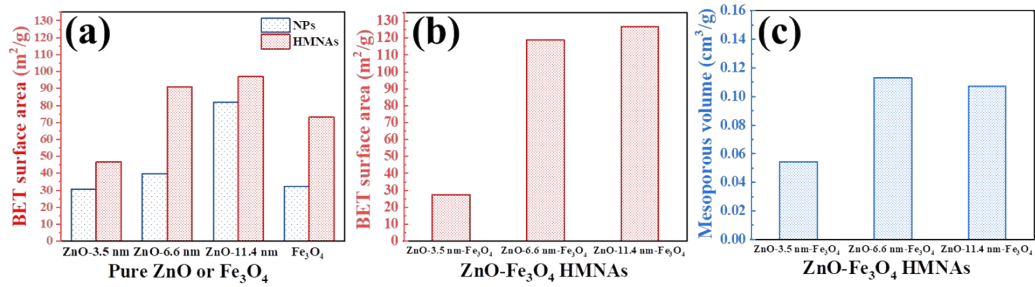


**Fig. S5.** BET surface areas of (a) ZnO NPs and HMNAs,  $\text{Fe}_3\text{O}_4$  NPs and HMNAs, (b) ZnO- $\text{Fe}_3\text{O}_4$  HMNAs obtained from different primary sizes of ZnO. (c) Mesoporous volumes of ZnO- $\text{Fe}_3\text{O}_4$  HMNAs.

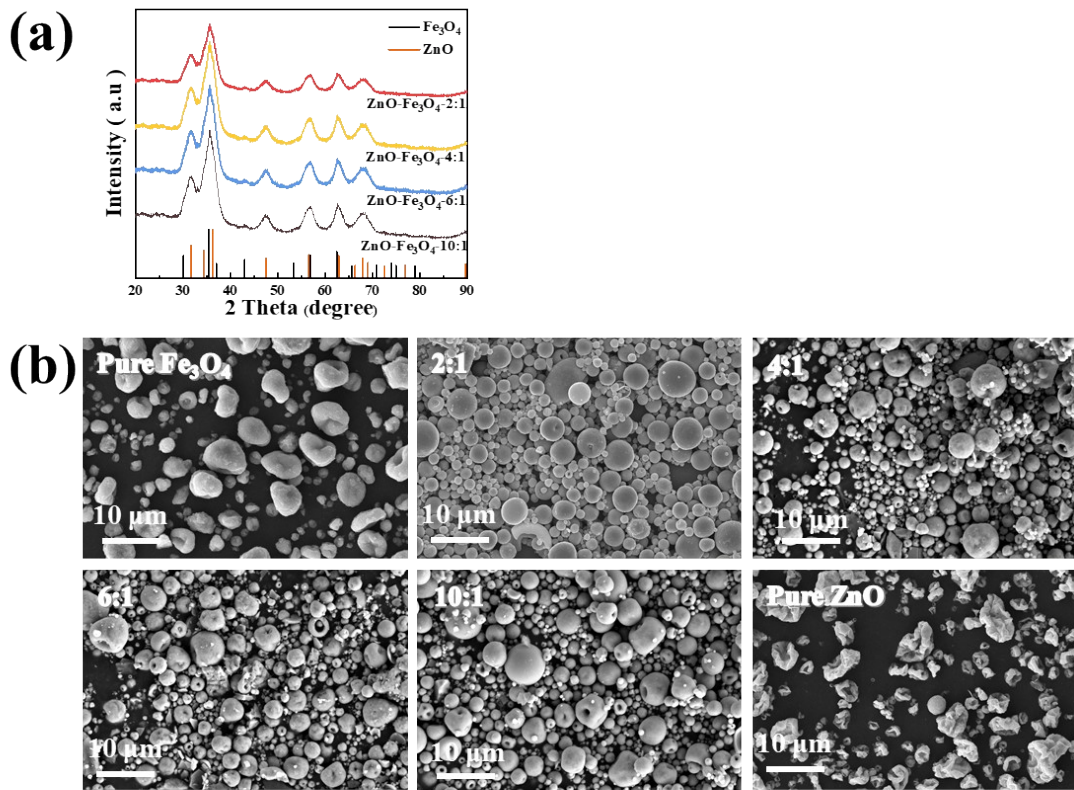


**Fig. S6.** (a) XRD patterns of ZnO- $\text{Fe}_3\text{O}_4$  HMNAs with different weight ratios of ZnO and  $\text{Fe}_3\text{O}_4$  NPs

and (b) SEM images.

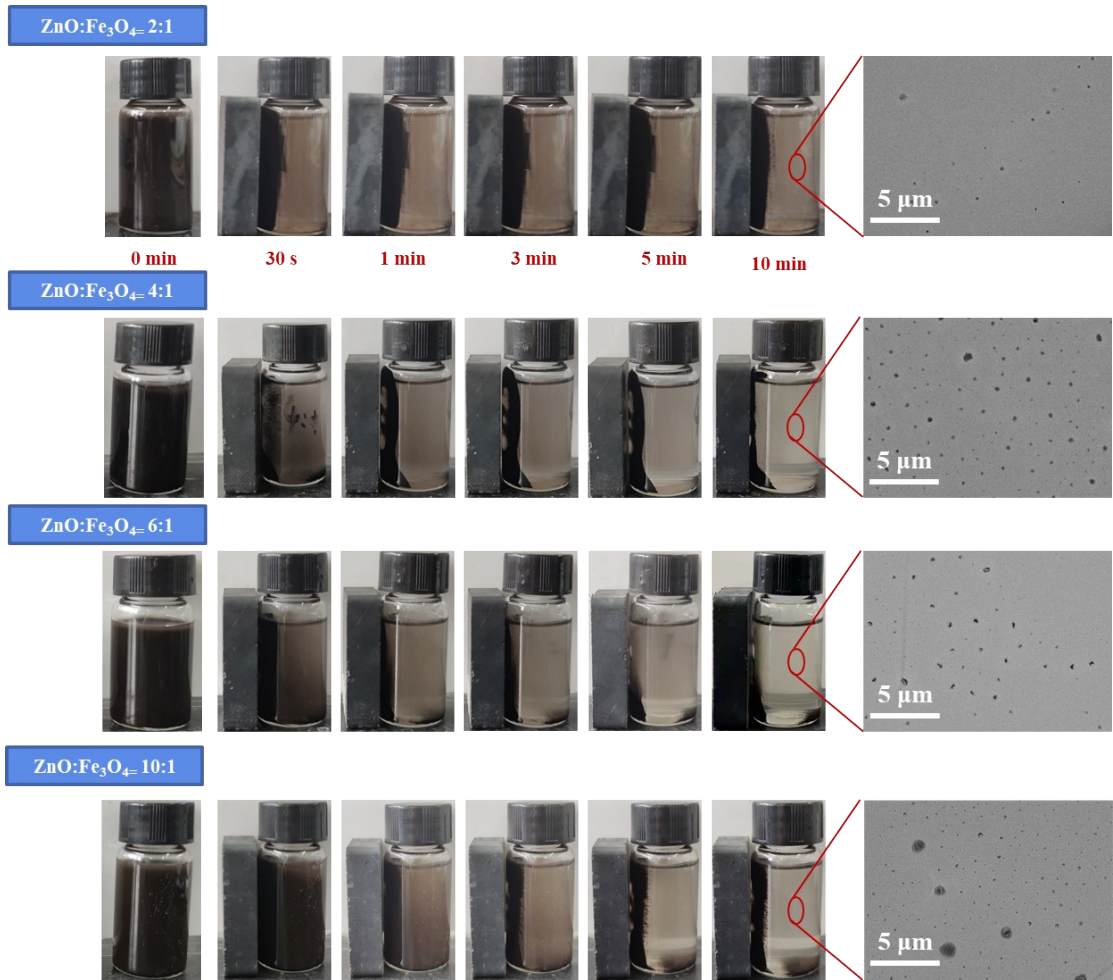


**Fig. S7.** Digital photographs of ZnO-Fe<sub>3</sub>O<sub>4</sub> HMNAs with different weight ratios of ZnO and Fe<sub>3</sub>O<sub>4</sub> NPs attracted to a magnet (3000 Gs).

attracted to a magnet (3000 Gs).

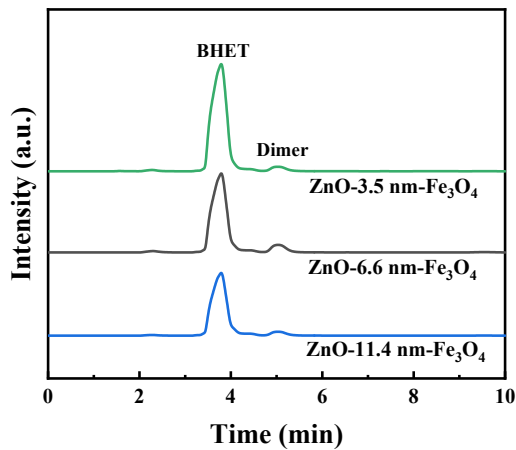


**Fig. S8.** HPLC chromatograms of the glycolysis products catalyzed by (a) ZnO-3.5 nm- $\text{Fe}_3\text{O}_4$  HMNAs, (b) ZnO-6.6 nm- $\text{Fe}_3\text{O}_4$  HMNAs, (c) ZnO-11.4 nm- $\text{Fe}_3\text{O}_4$  HMNAs.

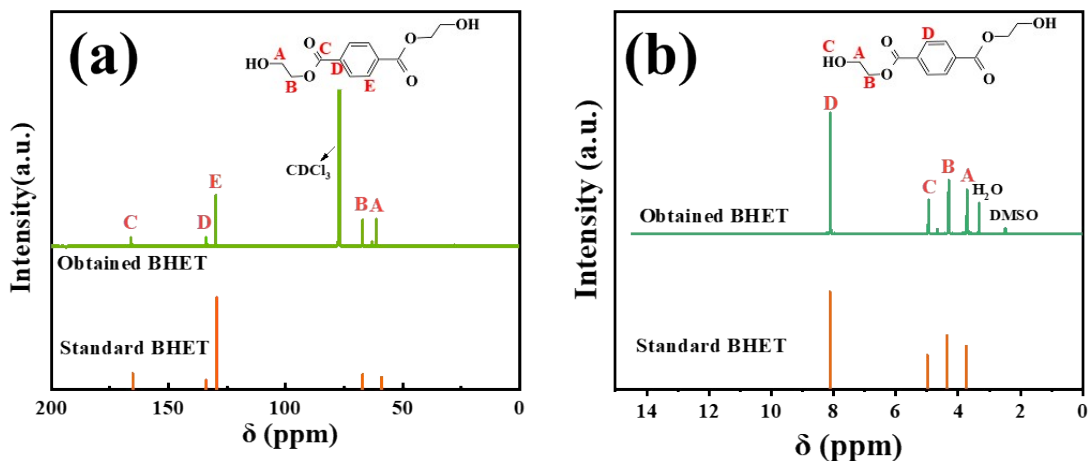


**Fig. S9.** (a)  $^{13}\text{C}$  NMR and (b)  $^1\text{H}$  NMR spectra of obtained BHET and standard BHET.

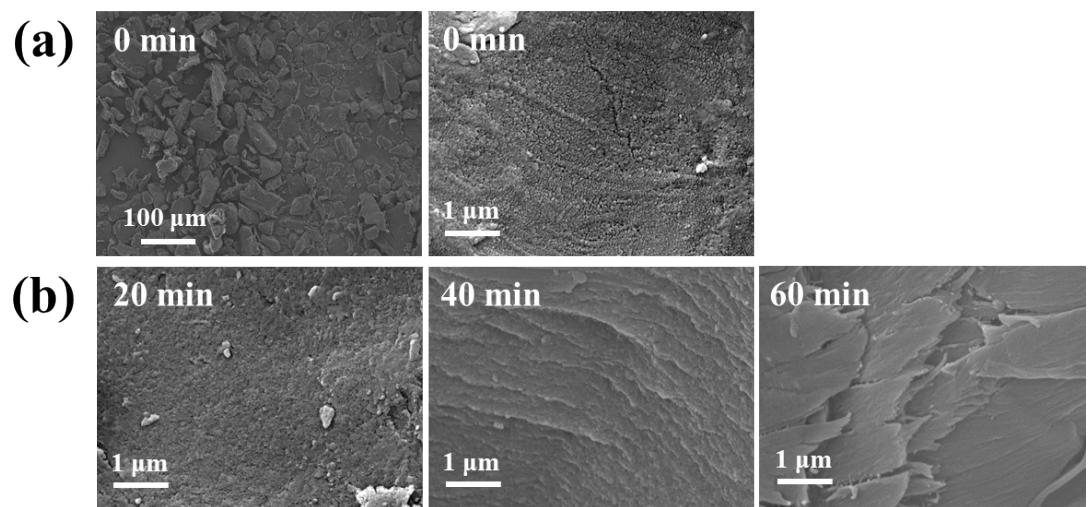


**Fig. S10.** SEM images of (a) virgin PET, (b) residual PET after the glycolysis for different times at 170 °C.

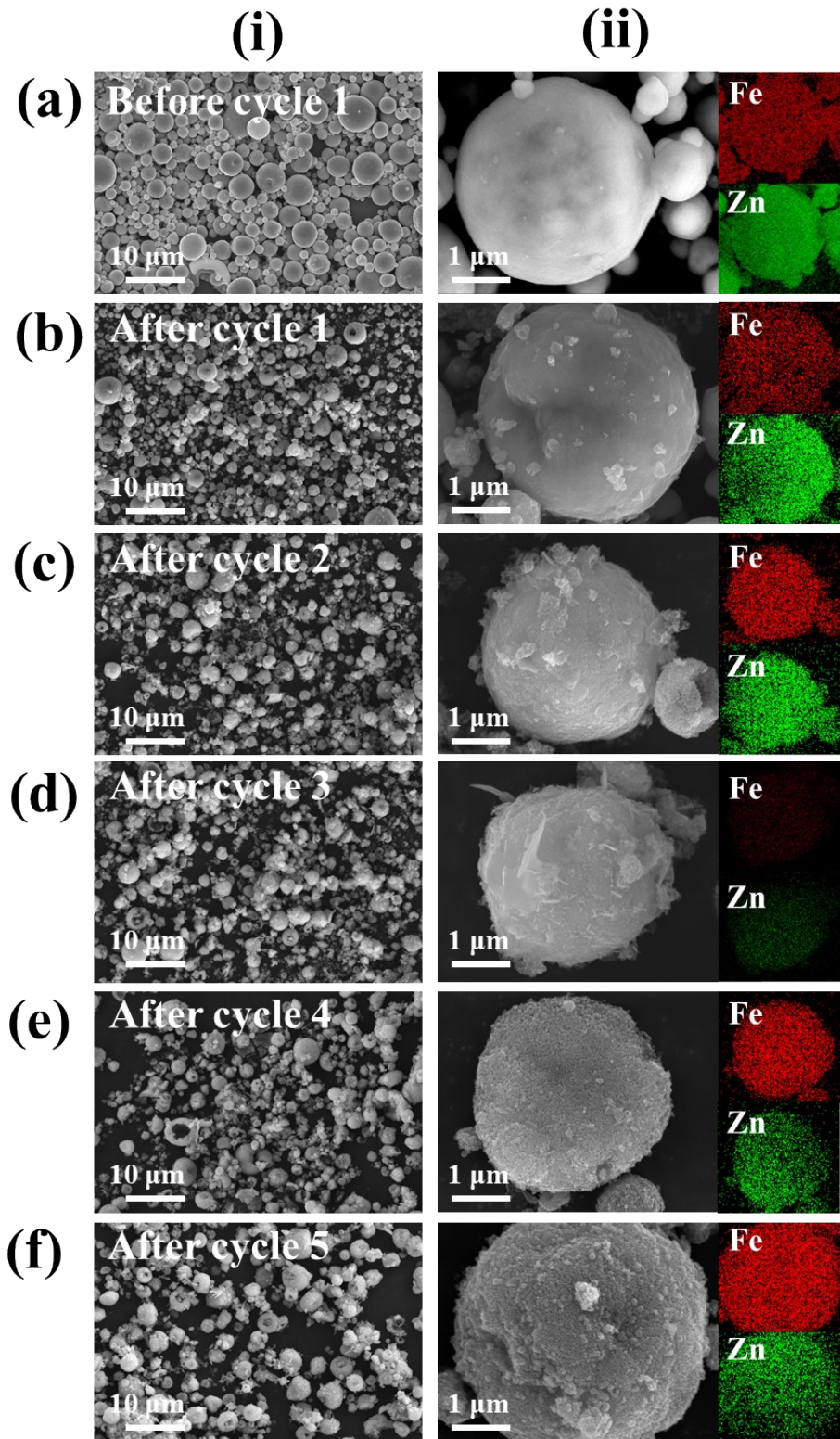


**Fig. S11.** SEM images, elemental mapping and EDS contents of Zn and Fe over the ZnO-Fe<sub>3</sub>O<sub>4</sub> HMNAs

before (a) and after each recycling step (b-f).

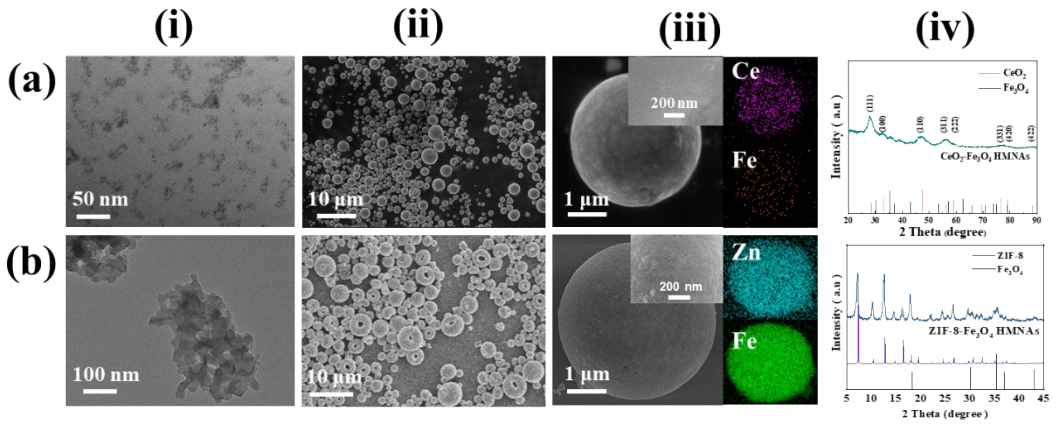


**Fig. S12.** (a) CeO<sub>2</sub>-2.7 nm and CeO<sub>2</sub>-2.7 nm-Fe<sub>3</sub>O<sub>4</sub>: (i) TEM image of CeO<sub>2</sub> nanoparticles. (ii-iii) SEM images of CeO<sub>2</sub>-2.7 nm-Fe<sub>3</sub>O<sub>4</sub> and elemental mapping. (iv) XRD patterns. (b) ZIF-8-30 nm and ZIF-8-Fe<sub>3</sub>O<sub>4</sub>: (i) TEM image of ZIF-8-30 nm. (ii-iii) SEM images of ZIF-8-30 nm-Fe<sub>3</sub>O<sub>4</sub> and elemental mapping. (iv) XRD patterns.

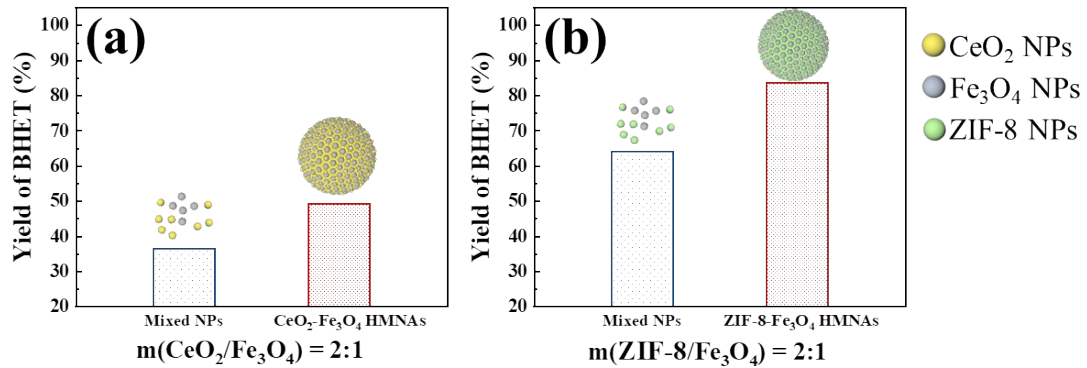


**Fig. S13.** (a) CeO<sub>2</sub>-2.7 nm and Fe<sub>3</sub>O<sub>4</sub> NPs directly mixed with the ratio of 2:1 and CeO<sub>2</sub>-Fe<sub>3</sub>O<sub>4</sub> HMNAs, (b) ZIF-8-30 nm and Fe<sub>3</sub>O<sub>4</sub> NPs directly mixed with the ratio of 2:1 and ZIF-8-Fe<sub>3</sub>O<sub>4</sub> HMNAs. (glycolysis at 180 °C, 40 min, the weight ratio of EG to PET of 6, catalysts of 1 wt%)

**Table S1.** Comparison of reported catalysts for the glycolysis of PET.

	Catalysts	Mass			Product		WHSV ( $\text{g}_{\text{BHET}} \cdot \text{g}_{\text{cat}}^{-1} \cdot \text{h}^{-1}$ )	Ref.
		ratio of cat./PET (%)	Temperature (°C)	Time (h)	yield (%)			
Nonmagnetic catalysts	ZnO/SBA-15	5	197	1	91	7.16	22	
	rGO\[TESPMI] <sub>2</sub> CoCl <sub>4</sub>	0.15	190	3	95.2	83.21	46	
	Graphitic carbon nitride colloid	2.5	196	0.5	80.3	25.27	12	
	MAF-6	1	180	4	81.7	8.03	45	
	Ultrasmall Co NPs	1.5	180	3	96	8.39	11	
	ZnO nanodispersion	0.7	170	1	82.3	46.24	13	
Magnetic catalysts	<b>ZnO-Fe<sub>3</sub>O<sub>4</sub> HMNAs</b>	1	190	0.5	92.3	72.61	This work	
	<b>CeO<sub>2</sub>-Fe<sub>3</sub>O<sub>4</sub> HMNAs</b>	1	197	0.75	95.39	50.03	This work	
	<b>ZIF-8-Fe<sub>3</sub>O<sub>4</sub> HMNAs</b>	1	190	0.33	85.2	101.55	This work	
	CoFe <sub>2</sub> O <sub>4</sub> @ZIF-8/ZIF-67	1	200	1	84.3	33.16	16	
	CoFe <sub>2</sub> O <sub>4</sub> /C10-OAC	2	195	2.5	95.4	7.50	43	
	$\gamma$ -Fe <sub>2</sub> O <sub>3</sub> /nitrogen-doped graphene	10	195	3	100	1.31	14	
	Mg-Al-O@Fe <sub>3</sub> O <sub>4</sub>	0.5	240	1.5	80	41.96	17	
	Zn-MNPs	0.8	196	2	79.8	19.62	44	
	Fe <sub>3</sub> O <sub>4</sub> NPs@h-BNNS	0.2	200	5	100	39.33	18	